Quantitative elasticity imaging by shear wave speed evaluation using inverse filtering

逆フィルタを用いた shear wave 速度推定による定量的弾性率イメージング

Yasunari Takayama‡, Kengo Kondo, Takeshi Namita, Makoto Yamakawa, and Tsuyoshi Shiina (Grad. School Med., Kyoto Univ.)
高山　裕成‡，近藤　健悟，浪田　健，山川　誠，椎名　毅（京都大院　医）

1. Introduction

Shear wave elastography can estimate the young's modulus of tissues by measuring shear wave speed and enables us to find diseases such as cancer or liver fibrosis in early stage by estimating tissue stiffness.[1] In shear wave elastography, acoustic radiation force (ARF) is used for generating shear wave in the body and shear wave propagation time is estimated by using time-of-flight method.[2] However, the method assumes the unidirectional propagation of shear wave and consequently genarates artifacts due to reflection and refraction wave.

We have proposed the method of obtaining shear wave speed by using inverse filtering. The method focuses shear waves by inverse filter and estimete shear wavelength by measuring the full width at half maximum of the focal point (FWHM).[3] As a result, the method can the estimate elasticity more accuracy because it does not need to assume the derection of shear wave propagation. On the other hand, FWHM is liable to underestimate shear wavelength due to the deformed pattern of focused shear waves.

In this work, we devided to introduce a shear wavelength compensation coefficient to correctly estimate shear wavelength in the practical condition. The performance of proposed method was validated with the homogeneous phantom and two-layered phantom experiment.

2. Methods of Elasticity Imaging

2.1 Overall flow

Figure 1(a) shows the schematic of plane shear wave exitation. Shear waves at θ degree propagate from 4 corners to the center of image plane. Assuming the shear waves obtained by each shear wave source is approximated as impulse responses, shear wave can be focused at arbitrary point by using inverse filter. In earlier study, wavelength was estimated by assuming FWHM is equivalent to half-wavelength (FWHM = $\lambda/2$).[4] In this study, we estimate the compensation coefficient by using simulation to correctly estimate shear wavelength. Shear wave speed c, is estimated by multiplying wavelength λ, by frequency f. Young's modulus are calculated by shear wave speed ($E = 3\rho c_s^2$). **Figure1 (b)** shows the flowchart of the proposed method.

2.2 Compensation coefficient to correctly estimate shear wavelength

Shear waves from all directions to the focal point are required to satisfy the condition that FWHM is equivalent to half-wavelength. However, in practice, the position or the direction of the plane shear wave excitation is restricted. **Figure 2** shows the pattern of focused shear waves at 300 Hz when the steering angles of plane shear wave θ, were set to three values as shown in Fig. 1(a); $\theta =$ [10°,15°,20°], [40°,45°,50°], [70°,75°,80°]. The focuses were simulated in the case of 25 kPa Young's modulus medium. Arrows in the Fig. 2 shows FWHM and wavelength ($\lambda/2$ = 4.81 mm) calculated by Young's modulus and frequency. In practice, when the steering degree was over $\theta = 20°$, side lobe effect arises. As a result, a pattern of focused shear wave in experiment was shaped like the long ellipse in the axial direction as shown in Fig. 2(a). In this case, the FWHM became smaller and, wavelength was estimated low. Then, to correctly estimate shear wavelength in the practical condition, we introduced a shear wavelength compensation coefficient $k_\lambda(f)$ which is defined as

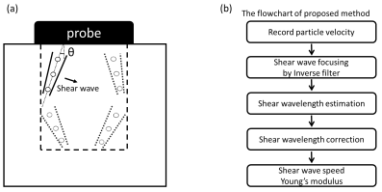

Fig. 1 (a) Schematic of the plane shear wave excitation, (b) flowchart of the proposed method.

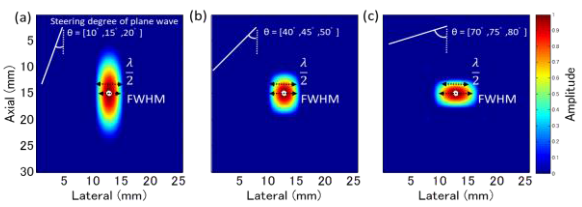

Fig. 2 Maps of the focused shear waves; (a) $\theta =$ [10°,15°,20°], (b) [40°,45°,50°], (c) [70°,75°,80°].

$k_\lambda(f) = \lambda(f) / \lambda'(f)$, where $\lambda(f)$ is the wavelength calculated from setting Young's modulus, and $\lambda'(f)$ is the wavelength estimated in simulation. Compensation coefficient $k_\lambda(f)$ was calculated for different values of Young's modulus at each frequency. Finally, the coefficient is multiplied by estimated shear wavelength in experiment to correctly estimate shear wavelength.

3. Experimental Condition

A modified Axiplorer (SuperSonic Imagine, France) ultrasound system with a 0.2 mm pitch 128-channel linear-array transducer (SL10-2, SuperSonic Imagine, France) was used for the proposed method. The center frequency was 5 MHz, and the frame rate was 5 kHz.

Three columnar phantoms (diameter 80 mm, height 60 mm) were used for experiment. They were homogeneous 0.8% agar phantom, homogeneous 1.2% agar phantom and two-layered phantom (soft layer: 0.8% agar, hard layer: 1.2% agar). We used dynamic mechanical analysis (DMA) to determine the young's modulus of these phantoms.

4. Experiment Results

Plane shear wave excitation steering at $\theta =$ [10°,15°,20°] was performed in experiment and simulation. **Figure 3** shows a result of calculation of compensation coefficients to correctly estimate shear wavelength at each frequency between 300 Hz and 600 Hz. These coefficients were averaged by 25, 50, 75, 100, 125 kPa Young's modulus because of little dependence on Young's modulus of simulation medium. **Figure 4(a)** is B-mode image. **Figure 4(b)** is an elasticity image of homogeneous (0.8%) agar phantom averaged between 300 Hz and 600 Hz. **Table I** shows Young's modulus of proposed method before and after correction, time-of-flight method, and DMA. Thanks to the compensation coefficient, quantitative performance of the proposed method has improved. The advantage of proposed method is estimating Young's modulus more quantitatively with less variation than time-of-flight method.

Figure 5(a) is B-mode image, and the boundary is located in 14 mm in axial direction. **Figure 5(b)** is averaged elasticity map. **Figure 5(c)** shows a profile of dashed line in Fig. 5(b). The red dashed line is the young's modulus estimated by DMA. The boundary of elasticity image was clear. However, complicated acoustic field reduced the accuracy of focusing and, Young's modulus estimated in both layer was different from DMA.

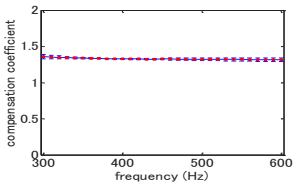

Fig. 3 Frequency dependence of compensation coefficients

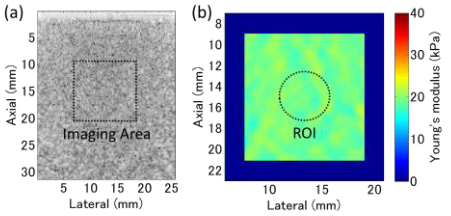

Fig. 4 (a) B-mode, (b) estimated elasticity image of homogenous phantom.

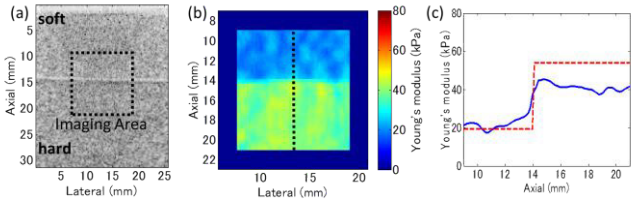

Fig. 5 (a) B-mode, (b) estimated elasticity image of two-layered elasticity phantom, (c) axial profile.

Table I Comparison of Young's moduli obtained by different methods

	Proposed		Time-of-flight	DMA
	After compensation	Before compensation		
0.8% agar (kPa)	19.3±0.9	10.9±0.5	20.3±1.4	19.3
1.2% agar (kPa)	47.1±2.3	26.7±1.3	58.7±4.6	53.8

The feasibility of proposed method was verified by homogenous and two-layered phantom.

5. Conclusions

We estimated the wavelength compensation coefficient by using simulation, and improved the accuracy of wavelength estimation in homogenous and two-layered phantom. Future works need to study focus pattern and wavelength estimation in complicated acoustic field to improve quantity performance of the proposed method.

References

1. A. Samani, J. Zubovits and D. Plewes: Phys. Med. Biol. **52** (2007) 1565.
2. M. Tanter, J. Bercoff, A. Athanasiou, et al.: Ultrasound in Med. & Biol. **34** (2008) 1373.
3. T. Kitazaki, K. Kondo, M. Yamakawa and T. Shiina: J. Appl. Phys. **55** (2014) 07KF10.
4. N. Benech, S. Catheline, J. Brum, et al.: IEEE Trans. Ultrason. Ferroelctr. Freq. Control **56** (2009) **2**400.